International Journal on
"Technical and Physical Problems of Engineering"
(IJTPE)
Published by International Organization of IOTPE

ISSN 2077-3528
IJTPE Journal
www.iotpe.com
ijtpe@iotpe.com

March 2022	Issue 50	Volume 14	Number 1	Pages 142-148

DESIGN OF FRAMELESS GIMBAL MOTOR FOR UAV APPLICATIONS

S. Arslan [1] I. Iskender [2]

1. Electrical and Electronics Engineering Department, Gazi University, Ankara, Turkey, arslansami@hotmail.com
2. Electrical and Electronics Engineering Department, Cankaya University, Ankara, Turkey, ires@cankaya.edu.tr

Abstract- Recently, application areas of the Unmanned Aerial Vehicle (UAV) systems have started to expand very rapidly due to the fact that offering more effective, economical, reliable and safe solutions compared to manned air platforms, satellites and/or various ground platforms. However, desire to develop higher performance, resourceful, lighter, small and low powered payload make the gimbal platforms mandatory part of the UAVs in a short time and their role is getting increased day by day. In parallel with the increasing demand for precise stabilization, robustness, lightness and agility in gimbal systems, it has become an important trend to use more-electric (ME) customed systems instead of traditional market products. The electric motors that control the speed and position of the gimbal system are simply referred to as gimbal motors. Related design study focuses on designing direct-drive in-runner frameless gimbal motor with the following features; 8.5 VAC line voltages, 24-slot/28-pole combination, 60 rpm, 80 mN.m. Permanent magnet synchronous motor topology is determined to offer higher torque density, higher precision and fast response required for gimbal platforms. The selecting criteria of dimensions, performance parameters, materials, machine type with rotor structures and motor duty cycle are also explained. The gimbal motor is performed analytically in Ansys RMxprt with parametric assignments, statistically and sensitively tuned in Maxwell 2D and optimized in Maxwell 3D by finite element method (FEM) optimetric convergence approach with magnetostatic and transient solutions to get the final machine shape. This study is currently part of the gimbal system to be produced for medium sized surveillance UAV. Since the gimbal motor has been prototyped, all dimensions given are valid.

Keywords: Gimbal, Permanent Magnet Synchronous Motor (PMSM), Surface Mount, Direct Drive, Finite Element Method (FEM), Frameless, UAV.

1. INTRODUCTION

A gimbal is simply defined as the pivoted platform that allows to control of an object rotating around the axis using an electric motor managed by a control system. The gimbal system is created by installing multiple gimbals on different axes. Gimbal systems have a wide range of usage areas at aerial photography, missile tracking, autonomous navigation, agriculture, robotics, mining and military to absorb the maneuvers, redundant motions, vibrations and nonlinear disturbances like frictions, rains, turbulences, mass unbalances and torque ripples that cause a decrease in the pointing accuracy of stabilization platform in order to hold steady the line-of-sight (LOS) [1]. A gimbal system are unique and specifically designed more based on the application and mostly comprises of gimbal and the driving sides. The gimbal side involve payload and target sensors whereas the driving side consists of electric motors, drivers and sensors to get rotation/angle information.

Because the specially mounted configuration of payload (here is located a quite sensitive featured thermal camera) mostly requires low volume, small size and high torque, it is very difficult or impossible to use commercial motors. The reason is that the commercially available gimbal motors are often designed for continuous load conditions and therefore they are generally over designed from the viewpoint of weight, volume and structure for such special applications. Besides, it is tedious to match the suited performance requirements like torque and speed with a commercially available motor. Since the performance of the gimbal drive system side directly affects the entire system, it is of great significance to design highly reliable and customed gimbal motor. Apart from smoothing and controlling angular movements, gimbal motors are mostly included in the category of servo motors due to the fact that they keep up the payload in the predefined position with defined rotation speed.

Some gimbal applications use power trains such as gear, belt or screw mechanisms. While the backlash in ratio-driven motor system makes precise positioning impossible, the disadvantages come with it cause increase in friction, complexity of mechanism and lower torsional resonance frequencies. On the other hand, direct-drive systems offer better torsional stiffness, less motion transmission errors and zero backlash [1].

In this study, the design procedure and optimetric analyses of low weight, low voltage, low speed direct-drive frameless brushless gimbal motor for yaw axis of triaxial gimbal system used in medium-sized surveillance UAV's are discussed in detail. The design starts with parametric solutions in RMxprt, where the input parameters are already calculated by macro based Octave calculations. Afterward, optimetric solutions are obtained by Maxwell 2D using statistical and sensitivity tools. Finally, design parameters are tuned over Maxwell 3D by using FEM.

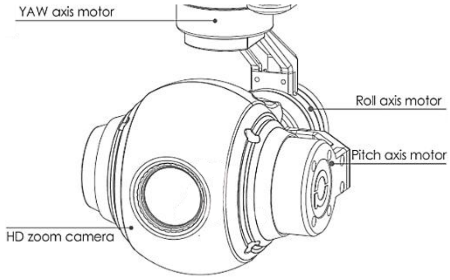

Figure 1. Three axis gimbal description

2. DESIGN CONSIDERATIONS

The gimbal motor to be designed has the size limitations listed in Table 1, which are mandated by the gimbal system manufacturer.

Table 1. Gimbal functional requirements

Limitations of Motor	Permitted Maximum Value
Outer Diameter, mm	106 (including mounted ear)
Mounted Ears	M2.5
Length, mm	20 (including winding)
Center of Mass Offset, mm	10
Total Mass, gr.	175

Rated torque and rated speed are given as 80 mN.m and 60 rpm respectively without efficiency criteria by the gimbal manufacturer. The acceleration and declaration time rate, payload mass, correction frequency, inertia of the platform and the center of mismatched mass are already considered. Gimbal motor operates in the range of 40 rpm and 110 rpm and inertia to be overcome is 17 g.m^2. Overload capacity is defined as 300% for duration of 1 min. Considering the overload capacity and the operating speed range, duty cycle is limited about to 50% for rated operation and the permissible maximum value of 95%.

Speed and the position of the gimbal motor can be measured by both incremental and absolute type encoders but the absolute one is preferred due to its capability of holding exact position even if power failure. Because the gimbal platform works at low and varying speed, encoder should meet robustness, anti-vibration, high temperature and highly sensitive features.

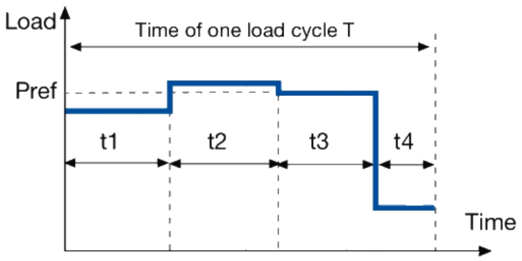

Figure 2. Gimbal motor duty cycle, S10

2.1. Machine Type Selection

The gimbal motor type is chosen to be competitive with high torque density, endurance and fast dynamic response features. Applicable motor types for gimbal applications are intensely limited due to size limitations and torque requirements:

1) Brushed dc motor, BDC
2) Reluctance synchronous motor, RSM
3) Switched reluctance motor, SRM
4) Stepper motor, SM
5) Brushless dc motor, BLDC
6) Permanent Magnet Synchronous Motor, PMSM

The PMSM type is offered for compactness, low maintenance, higher efficiency and torque density, better precision, lower noise and smoother torque [2]. For field application 3-phase PMSM is requested. Radially fluxed permanent magnet topology is preferred due to need of precision balancing and easy assembling.

In addition, the direct integration of the gimbal motor to the customed gimbal system has made it necessary to use a frameless structure which presents mechanical agility without the need for a shaft coupling and case. This contributes not only contributes reduction of weight but also reducing the costs. Except that it will be possible to increase inner diameter of stator which doubles the torque.

2.2. Stator and Rotor Type Determination

Combination of stator slots (S) per rotor poles ($2p$) has significant effect for winding layout, cogging torque and the space harmonics due to ampere-conductor distribution [2]. From the perspective of the designer, there is no the best design but optimum selection can be found by FEM analyses or be selected in the light of experience.

It is clear that increasing pole number until the limit of leakage flux which decreases the motor performance not only presents higher torque density for low speed gimbals but also reduces the required thickness of the rotor and stator yoke which offers weight advantage. By evaluating all these effects 24Slot/28Pole combination is based so that winding is concentrated with 0.966 winding factor [5]. Because maximum speed is limited to 110 rpm, drive frequency is 25.6 Hz, core loss is not matter.

PMSMs can be classified into in-runner and out-runner types in terms of stator-rotor position. Related gimbal drive region is suitable only for in-runner topology. Surface mounted and interior mounted PMs are very popular structures for PMSMs. Special mounted permanent magnet types are not generally preferred in gimbals due to high cost and construction difficulty.

For high pole numbered gimbal motor, surface mounted PM configuration offers simple structure, easy manufacturing, low torque ripple and low leakage flux [7]. So that the effect of reluctance torque developed by the variation of winding self-inductances can be neglected. Permanent magnet embrace is defined as the ratio of pole arc to pole pitch.

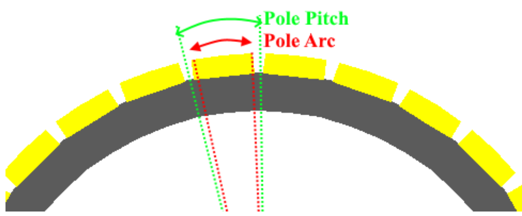

Figure 3. Surface-mounted permanent magnet rotor type and embrace

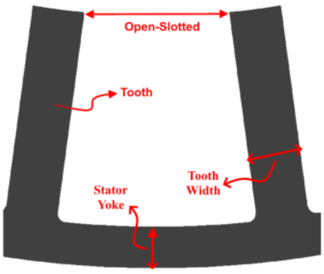

Figure 4. Open-slotted stator type

2.3. Predefined Parameter Definitions

Gimbal motor design begins with definitions of some acceptances. One of it is the specific electric loading (A) which defines the thermal characteristic of the motor and is determined by the stator current density J (A/mm^2), slot fill-factor (FF), the duty cycle (S) and the cooling type. For low speed and low powered gimbal applications, it can be limited to 10000-15000 A/m whereas typical electrical loading value is around 5000-30000 A/m depending thermal and cooling conditions. Furthermore, J, should be limited to 5-10 A/mm^2 by considering the gimbal motor operates at high altitude [2].

2.3.1. Duty Cycle

Duty cycle defines the operating load conditions of the electric motors defined by IEC (International Electrotechnical Commission) including working sequences. Duty cycle for gimbal motor is already defined as S-10 by gimbal manufacturer as in Figure 2 (t_1= 1 ms, t_2= 2.5 ms, t_3= 0.5 ms, t_4= 1 ms).

As thought the correction time is too less and gimbal motor has nominal load only at the half of load period, the current density J can be examined at edge of 10 A/mm^2 for this application.

2.3.2. Slot and Winding Type

It is clear that number of turns should be comparatively high to get the correct EMF for low speed motors such as gimbal motors and mostly it is hard to make such winding and results low slot fill factor. Therefore, winding type directly affects the stator slot type which affects the performance [4] of the gimbal motor in addition to air-gap flux density and cogging torque, should be careful decided. To overcome these challenges, mould based winding technique and open-slotted stator type is preferred as in Figure 4.

2.3.3. Slot Fill Factor (*FF*)

Slot fill factor determines how much copper can be packed into the stator slot and is directly related with winding method, slot type and experience. By considering that stator will has open slotted type, coated insulating instead of press-bands and mold wound concentrated winding, slot fill factor is limited to 40%-45%.

2.3.4. Materials

Stator and rotor core materials are chosen based on limitations of the saturation level, iron losses and the cost [5]. Mostly non-grain oriented electric steel is preferred for stator and rotor, because of isotropy and cost. But especially for low speed gimbal motors rotor material may be replaced with massive magnetic steel.

For the rotor magnets, although SmCo magnets have a high curie temperature, NdFeB magnets are more prominent for gimbal motors because of their higher unit volume power densities, higher remanence, higher coercivity, lower density and higher tensile strength.

2.3.5. Air-Gap Clearance

Air-gap length directly affects the air-gap flux density and depends on mostly mechanical issues such as production methods and tolerances. Even if a longer air-gap length compensates mechanical effects but results with thicker PM which increases leakages to keep air-gap flux density same at that volume. For convenience and in the light of factory production capabilities, air-gap length is defined as 1 mm.

3. ANALYTICAL SOLUTIONS

The gimbal motor design study begins with Octave macro based analytical dimensioning basis of [3]. Outputs of Octave calculations are input to RMxprt for parametric solutions. Outputs of RMxprt are input to Maxwell 2D for statistical and sensitive tools. Outputs of Maxwell 2D are input to Maxwell 3D for final optimetric convergence approach. Gimbal motor model is splitted by quarter using symmetry features of gimbal motor to reduce FEM solution duration. Boundary conditions are assigned as Master and Slave. Fields are bordered with zero vector potential. Design flow is illustrated in Figure 5.

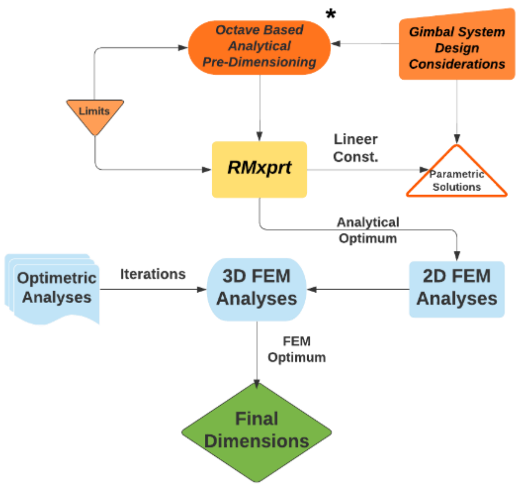

Figure 5. Design study flow

3.1. Octave Based Macro Outputs

Octave based preliminary dimensions are listed elementarily in Table 2. System constraints are already defined. Frictional and windage loss is estimated as 40 mW. Stator skew is offered as 0.5 slot pitch because the model depth is too short and is not feasible for magnet skewing. Specific electric loading (A) is kept at 20000 A/m whereas air-gap flux density (T) at 0.6 T. For stator M310-50 stainless steel, for rotor AISI 1020 and for magnets N45H material is assigned for initial analytical calculations.

Table 2. Octave macro based preliminary dimensions

Stator Data	
$D_{in}^2 L$	44800 mm^3
L	7 mm - selected
D_{in}	80 mm - selected
D_{out}	101 mm
Tooth width	3.5 mm
Tooth height	8 mm
Yoke	2.5 mm
Rotor Data	
Air-gap	1 mm
R_{out}	78 mm
V_{mag}	4949 mm^3
T_{mag}	3 mm
Magnet embrace	1
Yoke	4.5 mm
Winding Data	
cps	250
wd	0.40 (0.05 mm wrap)
J	9 A/mm^2
FF	45%
Parallel branch / strands	1 / 1
Total Net Weight	
240 gr	

Because low weight is primary goal for the system, D_{in}/L ratio should be as high as possible by taking consideration into the inertia since efficiency is at background. Keeping that the allowable motor length is 20 mm including winding, stator length is selected as 7 mm for safety wound. So, D_{in} can be calculated as 80 mm. Allowable D_{out} of motor is 106 mm including 2.5 mm mounting holes so the stator outer diameter is selected 101 mm. Analytically calculated efficiency is around 6%.

Table 3. Summarized performance data

General Data of Gimbal Motor (Summarized)	
Nominal power	500 mW
Nominal torque	80 mN.m
Nominal speed	60 rpm
Speed range	(40-110) rpm
DC bus voltage	24 VDC
Rated phase voltage	4.9 VACrms
Overload capacity	300% (1 min)
Stator slot / rotor pole	24S / 28P

3.2. RMxprt Parametric Solutions

RMxprt analyses are performed based on parametric and optimetric assignments. Unusually, the stator design begins from outer to inner radius instead of from inner to outer because of the system has maximum diameter limitation. It is very hard to investigate all graphs but it is effective to study significant ones. All data is summarized in Table 4 and efficiency is increased up to 9.7% in RMxprt by parametric solutions.

3.2.1. Airgap Flux Density

Unlike the specific electric loading (A), the specific magnetic loading (B) defines average air-gap flux density and has less adjustable range due to limitations of material saturation and core losses. So, for gimbal motor air-gap flux density will be limited to 0.5-0.6 T.

Higher torque density can only be obtained by working on saturation limits of specific magnetic and electric loadings. Although stator yoke thickness can be reduced up to 1.8 mm where yoke flux density is around 1.75 T, because of producibility 2.5 mm needs to be selected, similarly, 4 mm for rotor yoke is required for producibility.

Table 4. RMxprt based dimensions (FEM Input)

Stator Data	
D_{out}	101 mm
D_{in}	75 mm
L	5 mm
Tooth width	2.5 mm
Tooth height	10 mm
Stator yoke	2.5 mm
Rotor Data	
Air-gap	1 mm
R_{out}	73 mm
T_{mag}	2.3 mm
Magnet Material	N45H
Magnet embrace	0.7
Yoke	4 mm
Winding Data	
cps	294
wd	0.40 (0.05 mm wrap)
J	5.8 A/mm^2
FF	40%
Parallel branch / strands	1 / 1
Total Net Weight	
152 gr	

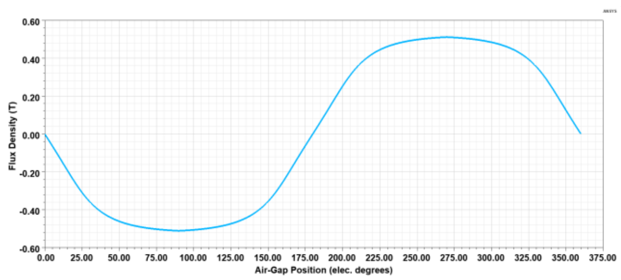

Figure 6. Airgap flux density vs airgap position in electrical degree

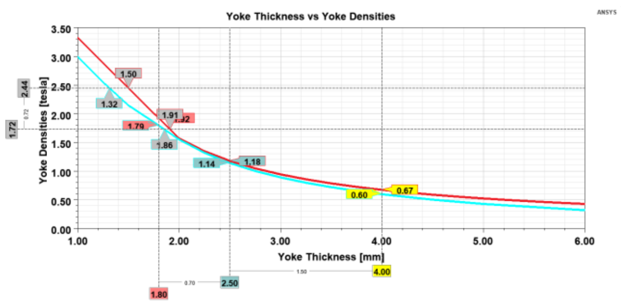

Figure 7. Yoke thickness vs yoke flux densities

3.2.2. Stator Slot Height

Since the outer diameter for gimbal motor is limited to 101 mm without mounting ears, the inner diameter of the stator and the slot height (H), which affects the number of turns per slot and the wire diameter, are selected in the light of the motor weight. The optimum power to weight ratio is obtained when L is 5 mm and H is 10 mm. So inner diameter of the stator corresponds to 75 mm.

3.3. Maxwell 2D FEM Solutions

Maxwell 2D FEM analyses of the gimbal motor are based on its optimetric solutions using statistical and sensitivity tools. FEMs are powerful and sensitive tool in the analyses and design of special electric machines.

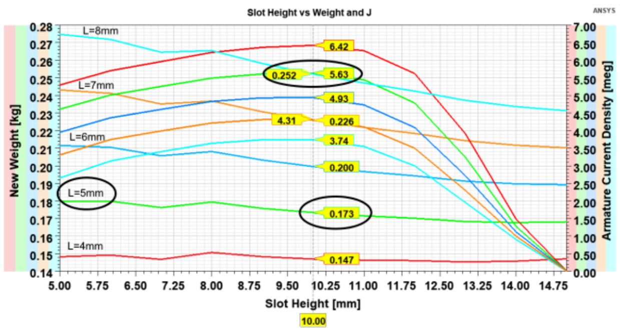

Figure 8. Slot height vs net weight and current density

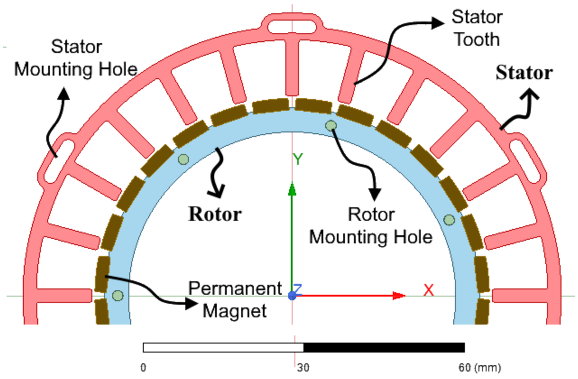

Figure 9. 2D model of gimbal motor

3.3.1. Induced Phase Voltages

Open-slot type stator is used to increase stator slot fill factor and winding manufacturability although it decreases teeth flux density. Harmonics of induced voltages can be reduced with the further effort of optimizing teeth and permanent magnets shape.

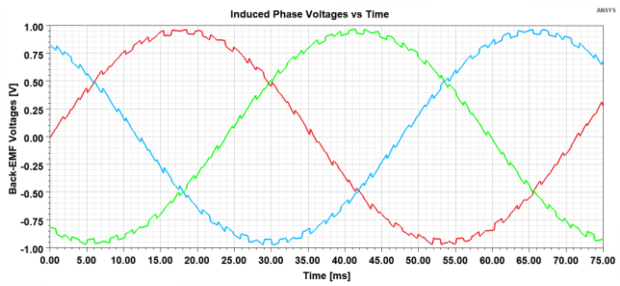

Figure 10. Induced phase voltages

3.3.2. Statistics

The statistical tool is a type of parameter filter for investigating the effects of an input parameter population on output performance whereas sensitivity tool tunes the design outcomes to meet cost functions. However the design parameters filtered by statistics are further tuned by using sensitivity tool to get optimetric solutions.

For statistical analysis, the length of the gimbal motor, the embrace and thickness of magnets, the height of the slots, the tooth width and the rotor yoke were selected as the population outputs. The outcomes meet the maximum output capability of the gimbal motor is 300%, are investigated.

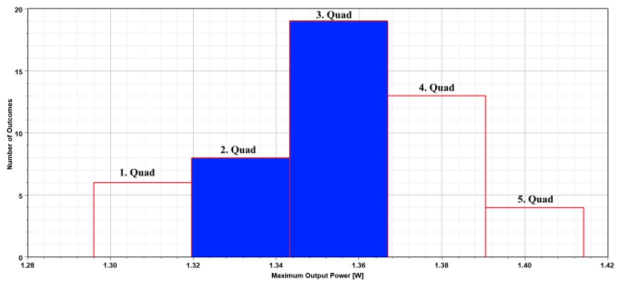

Figure 11. Outcomes vs output power statistics

For the gimbal motor maximum output power is required minimum 1.3 W. However, the current density at rated is expected to be maximum 6 A/mm^2. The outcomes satisfying the requirement lay on the 2nd and 3rd quadrants.

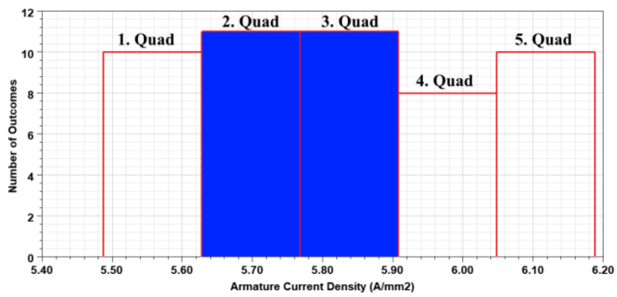

Figure 12. Outcomes vs current density at rated statistics

3.3.3. Flux Densities

Stator yoke, stator teeth and rotor yoke flux densities are inside the limits and designed gimbal motor is far from saturation. For the stator saturation point is defined as 1.72T whereas for rotor it is 2.5 T.

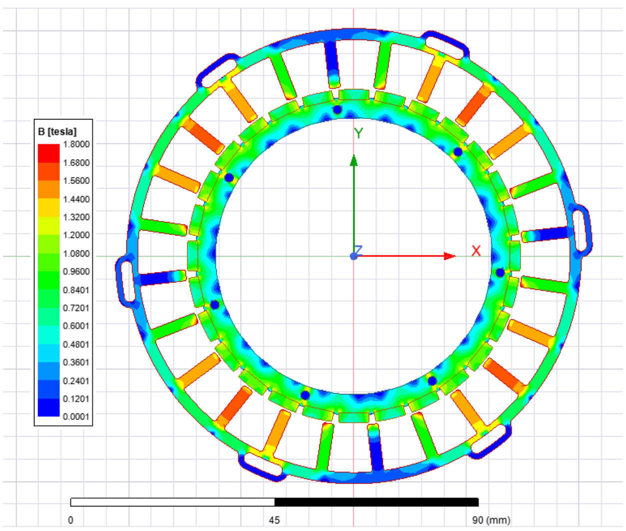

Figure 13. Gimbal motor flux densities in 2D FEM

3.4. Maxwell 3D FEM Solutions

Maxwell 3D solutions are based on optimetric convergence approach with magnetostatic and transient solutions to get the final machine shape using the FEM.

3.4.1. Pole Embrace vs Cogging Torque

Cogging torque, also called as detent torque, is caused by the attraction of the rotor magnets and the stator steel teeth. In the presence of cogging, rotor tries to align itself to minimum energy point which reduces driver performance mostly at light load and low speed especially in gimbal applications. Therefore, the elimination of the cogging torque is important for gimbal applications.

Pole embrace also directly affects the back-emf voltages and cogging torque, it is important to find optimum point of it, here it is 0.7.

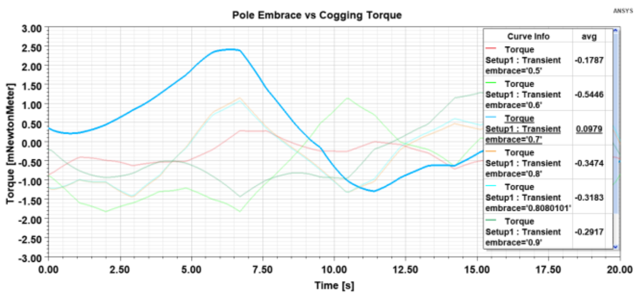

Figure 14. Pole embrace vs cogging torque

Some techniques are introduced in literature [3] to reduce cogging torque. However, it is difficult to skew rotor magnets for the gimbal motors which has very short model depth so that stator skew is more applicable. So, for the model, 0.5 slot pitch skew is achieved.

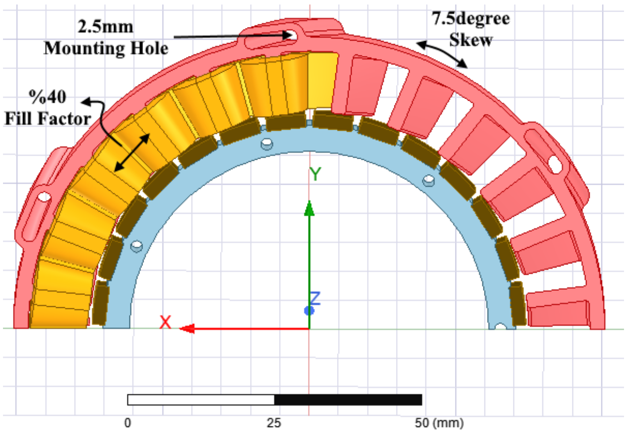

Figure 15. Skewing of stator (0.5 slot pitch)

Besides that, high pole numbered gimbal motors have smaller pole pitch which corresponds to shorter end turns offers less resistive loss, which increases efficiency and decreases the thermal management burden [3].

3.4.2. Current Density

The current density can be increased up to 9 A/mm^2 for rated operation and to 16 A/mm^2 for maximum power operation. Tooth width is adjusted until J will be 6 A/mm^2 at rated load conditions which is inside the limits. Besides, J analyzed by 3D FEM is around 11 A/mm^2 at maximum run that is enough for gimbal motor to meet 1 min 300% overload expectation comfortably.

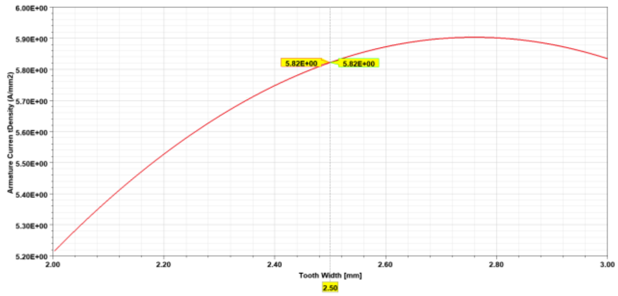

Figure 16. Tooth width vs armature current density in 3D FEM

Because the current density is far more behind the limits, fill factor can be increased up to 40% to reduce winding problems such as loose wires and short-circuit failures [6].

3.4.3. Output Torque

Permanent magnet properties are affected by temperature exponentially so the torque generated. For safety, the permanent magnet design is based on the properties of the magnet material at 80 degrees. Designed gimbal motor provides nominated torque 80 mN.m with 2.6% ripple that is inside the limits. Whereas, maximum output power is 1.4 W with 0.8% torque ripple that is inside the limits as seen in Figure 18.

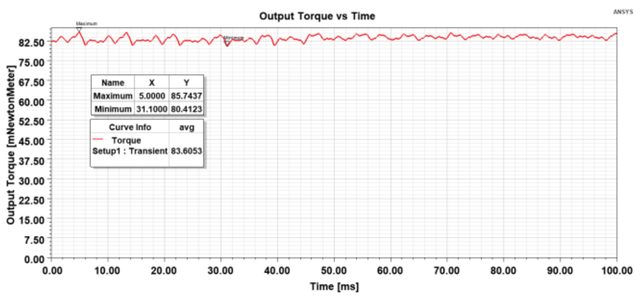

Figure 17. Rated output torque vs time in 3D FEM

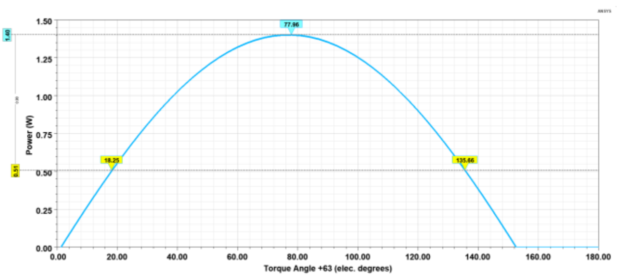

Figure 18. Torque angle vs output power

4. CONCLUSIONS

The design of low voltage low speed direct-drive frameless in-runner gimbal motor is performed. The design criteria such as material type, machine topology, rotor and stator structures are explained. Electric and magnetic solutions of the gimbal motor are analyzed analytically in Ansys RMxprt and optimized in Maxwell 2D&3D by finite element method. There is remarkable difference between Octave based analytical designs and software based analytical designs (RMxprt).

Furthermore, 2D FEM results are close to analytical ones in RMxprt except the solutions effected by non-linearity. So, the effect and importance of the FEM tools while designing gimbal motor is felt. To reduce cogging torque, ripples and the harmonics, stator skewing is applied. The design work then proposes to determine aspect ratio for the gimbal system, so that generalized studies can be easily applied to multi-degree freedom systems. Optimization techniques are also available for further performance improvements.

APPENDICES

Appendix 1. Nominal and Maximum Line Voltages

PWM technique is Space Vector Pulse Width Modulation (SVPWM). DC bus voltage = 24 VDC. Gimbal motor nominal speed is 60 rpm whereas maximum speed is 110 rpm. Nominal line voltage is calculated as $24\ \text{VDC}/\sqrt{2}\times 0.95\times 0.53 = 8.5\ \text{VACrms}$, maximum line voltage is as $24\ \text{VDC}/\sqrt{2}\times 0.95 = 16\ \text{VACrms}$.

NOMENCLATURES

1. Acronyms

UAV	Unmanned Aerial Vehicle
FEM	Finite Element Method
PMSM	Permanent Magnet Synchronous Motor
FOC	Field Oriented Control
SVPWM	Space Vector Pulse Width Modulation

2. Symbols / Parameters

A: Specific electric loading in A/m
B: Specific magnetic loading in T
J: Current density in A/mm^2
D_{in}: Stator inner diameter
D_{out}: Stator outer diameter
L: Length
R_{out}: Rotor outer diameter
V_{mag}: Permanent magnet volume
w_d: Wire diameter
T_{mag}: Permanent magnet thickness
cps: Conductors per slot
H: Stator slot height
S: Gimbal motor duty cycle

ACKNOWLEDGEMENTS

This work is supported by Promethod Engineering Ind. Trade. Co. Ltd. in Turkey. The analytical designs and FEM analyses are performed by using licensed usage of Ansys Electronics, Maxwell, RMxprt and 2D, v2021R1, respectively.

REFERENCES

[1] G. Ozdogan, K. Leblebicioglu, "Cogging Torque Disturbance Rejection for a Low-Cost Gimbal Motor and a Controller Design with Practical Considerations", The 12th Asian Control Conference (ASCC), pp. 486-491, 2019.
[2] J.R. Hendershot, "Design of Brushless Permanent-Magnet Machines", Venice, Florida: Motor Design Books.
[3] C.D. Hanselman, "Brushless Permanent Magnet Motor Design", 2 Edition, Magna Physics Publishing, ISBN: 1-881855-15-5, USA: Lebanon, 2003.
[4] H. Vu Xuan, D. Lahaye, H. Polinder, J.A. Ferreira, "Influence of Stator Slotting on the Performance of Permanent-Magnet Machines with Concentrated Windings", IEEE Transactions on Magnetics, Vol. 49, No. 2, pp. 929-938, Feb. 2013.
[5] S. Arslan, I. Iskender, "Design aspects of a 26500-rpm: 2-kw High-Speed Permanent Magnet Synchronous Generator for Turbomachinery Systems", 8th International Conference on Electronics, Computers and Artificial Intelligence (ECAI), pp. 1-6, 2016.
[6] M. Iorgulescu, "Study Relation Between Fault Noise in Electric Motor", International Journal on Technical and Physical Problems of Engineering (IJTPE), Issue. 5, Vol. 2, No. 4, pp. 69-73, December 2010.
[7] M. Ebadpour, M.B.B. Sharifian, "Cost Effective Current Control and Commutation Torque Ripple Reduction in Brushless Dc Motor Drives", International Journal on Technical and Physical Problems of Engineering (IJTPE), Issue. 18, Vol. 6, No. 1, pp. 154-159, March 2014.

BIOGRAPHIES

Sami Arslan was born in Isparta, Turkey on May 21, 1990. He received the B.Sc. degree in Electrical and Electronics Engineering, Gaziantep University, Gaziantep, Turkey in 2012 and M.Sc. degree in Electrical and Electronics Engineering, Gazi University, Ankara, Turkey in 2014, where he is currently pursuing the Ph.D. degree. His research interests are permanent-magnet machines, design and optimization of electrical machines and power electronics.

Ires Iskender received his M.Sc. and Ph.D. degrees in Electrical Engineering from Middle East Technical University Ankara, Turkey in 1991 and 1996, respectively. From 1997 to 2017 he worked as a Teaching Fellow at the Electrical and Electronics Engineering Department of Gazi University. Since 2018 he has been with the Department of Electrical and Electronics Engineering Department, Cankaya University Ankara, Turkey where he is currently a Professor. His research interests include energy conversion systems, renewable energy sources, electrical machine, and power quality.